Thermal Characteristics of Liquid Metal Interconnects for Power Semiconductors

Original
Thermal Characteristics of Liquid Metal Interconnects for Power Semiconductors / Sun, Z., Bjorn Jorgensen, A., Baker, N., Beczkowski, S., Guo, W., Munk-Nielsen, S., Iannuzzo, F.. - ELETTRONICO. - (2023), pp. 1135-1140. (APEC 2023 - 38th Annual IEEE Applied Power Electronics Conference and Exposition Orlando (United States) 19/03/2023 - 23/03/2023) [10.1109/APEC43580.2023.10131435].

Publisher:
IEEE (Institute of Electrical and Electronics Engineers)

Published
DOI:10.1109/APEC43580.2023.10131435

Thermal Characteristics of Liquid Metal Interconnects for Power Semiconductors

Sun, Zhongchao; Jorgensen, Asger Bjorn; Baker, Nick; Beczkowski, Szymon; Guo, Wendi; Munk-Nielsen, Stig; Iannuzzo, Francesco

Published in:
APEC 2023 - 38th Annual IEEE Applied Power Electronics Conference and Exposition

DOI (link to publication from Publisher):
10.1109/APEC43580.2023.10131435

Publication date:
2023

Document Version
Accepted author manuscript, peer reviewed version

Citation for published version (APA):
Sun, Z., Jorgensen, A. B., Baker, N., Beczkowski, S., Guo, W., Munk-Nielsen, S., & Iannuzzo, F. (2023). Thermal Characteristics of Liquid Metal Interconnects for Power Semiconductors. In *APEC 2023 - 38th Annual IEEE Applied Power Electronics Conference and Exposition* (pp. 1135-1140). Article 10131435 IEEE (Institute of Electrical and Electronics Engineers). https://doi.org/10.1109/APEC43580.2023.10131435

Thermal Characteristics of Liquid Metal Interconnects for Power Semiconductors

Zhongchao Sun
AAU Energy
Aalborg University
Aalborg, Denmark
zs@energy.aau.dk

Asger Bjørn Jørgensen
AAU Energy
Aalborg University
Aalborg, Denmark
abj@energy.aau.dk

Nick Baker
Department of Electrical and Computer Engineering
The University of Alabama
AL, USA
nbaker2@ua.edu

Szymon Beczkowski
AAU Energy
Aalborg University
Aalborg, Denmark
sbe@energy.aau.dk

Wendi Guo
AAU Energy
Aalborg University
Aalborg, Denmark
wg@energy.aau.dk

Stig Munk-Nielsen
AAU Energy
Aalborg University
Aalborg, Denmark
smn@energy.aau.dk

Francesco Iannuzzo
AAU Energy
Aalborg University
Aalborg, Denmark
fia@energy.aau.dk

***Abstract*—Due to its electrical conductivity and fluidity, liquid metal interconnection has the potential to become a new industrial power semiconductors packaging application method to solve the failure of wire bonding liftoff and improve the reliability of power semiconductor applications. As a crucial characteristic in use, the thermal characteristics of liquid metal interconnects for power semiconductors are obtained experimentally in this paper. By powering a diode die in a bridge busbar liquid metal interconnect structure, the thermal resistance from the die to the ambient is extracted. The result shows that the liquid metal interconnects method has the potential to improve the thermal behavior of power semiconductors compared with wire-bonding interconnection. The finite element simulation explains the possible reasons causing abnormal temperature responses among some samples. Besides, during the test, a slow decline in the forward voltage of the module is observed.**

Keywords—liquid metal, wire-bonding, thermal characteristics, packaging, simulation

I. INTRODUCTION

Because of the critical role power semiconductors play in modern industrial applications, ensuring the reliability of power modules is of great importance to manufacturers and consumers. Wire bonding is the most common interconnection method for power semiconductors (Fig.1a) [1], while due to the different coefficients of thermal expansion of bond wires and semiconductors, the bond wires usually become the weakest failure points in power modules because of lift-off [2]. Liquid metals (LMs) are promising functional materials due to their unique combination of fluidity and metallic properties at room temperature [3]. For power semiconductors packaging, LM can constitute the electrical connection between the semiconductor and outer circuits and replace the functions of bond wires. A benefit of the fluidity of LM at room temperature is that there is no crack initiation and propagation, so it has a stronger ability to resist thermo-mechanical stress. Taking this advantage, Nick Baker et al. [4] manufactured the LM interconnect prototype using liquid gallium, as shown in Fig. 1b. The initial thermal cycles test on it shows the LM-interconnect diode has up to 5x to 10x longer lifetime than the wire-bond diodes and the thermo-mechanical related failure of the interconnection was completely removed.

With the development of power semiconductors towards high power density, the working junction temperature of semiconductors continues to increase, and good thermal characteristics of package design are an important factor in ensuring the stable and safe operation of semiconductor devices. Because the morphology of LM in the package structure is affected by factors such as surface tension, surface oxidation, and wetting characteristics relative to surrounding materials [5], the thermal characteristics of LM interconnects in practical use are different from heat conduction in solids of conventional packages.

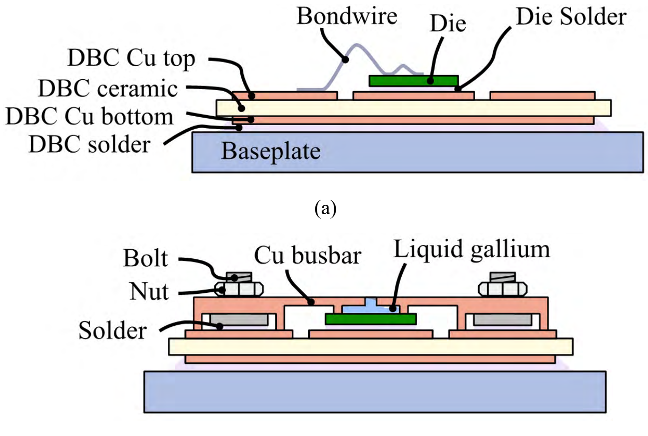

(a)

(b)

Fig. 1. Structure of power semiconductors interconnects by, (a) bond wire, (b) liquid metal.

In this paper, the thermal characteristics of the LM interconnect for power semiconductors are experimentally demonstrated and compared with wire-bonding interconnections. Additionally, the phenomenon of forward voltage decreasing is observed and discussed to support the application potential of LM interconnects. Based on the experimental results, possible factors that might affect the thermal behavior of LM interconnects are proposed and evaluated by simulation.

II. METHODOLOGY

Similarly to the approach described in [6], to obtain the thermal characteristic of the LM interconnections for power semiconductors and compare it with the wire-bonding method, the input power is applied to the device near the interconnect structure, and the temperature response as a function of time is measured. The transient thermal resistance from the device to the ambient based on its power dissipation is calculated as

$$Z_{th}(t) = \frac{T(t) - T_a}{P(t)} \tag{1}$$

where Z_{th} is the device transient thermal resistance, T is the device temperature, T_a is the ambient temperature and P is the device power dissipation.

(a)

(b)

Fig. 2 Experiment samples, (a) wire-bonding interconnection (sample 0), (b) liquid metal interconnection (samples 1-3).

III. EXPERIMENT

A. Samples

The traditional wire-bonding interconnection module with 350 µm diameter aluminum bond wires is shown in Fig. 2a, marked as sample 0. Instead of using bond wires, the LM-interconnect solution connects the diode die to a copper bridge busbar by liquid gallium, where the busbar terminals are fixed to the DBC by bolts, as shown in Fig. 2b. Three samples marked as samples 1-3 were prepared.

B. Temperature measurement

The temperature measurement setup is shown in Fig. 3. The module is fixed on a large aluminum heatsink whose temperature is regarded as the ambient temperature and the diode die is the active component powered by a DC power supply SM66-AR-110. The input current is increased in steps from 10.0A to 80.0A. The power dissipation of the module is calculated by multiplying the input current and the voltage read from the power supply. Three fiber optic temperature sensors are used to measure the surface temperatures of the LM, diode die, and heatsink, which are extracted and recorded by an Opsens 8-channel signal conditioner. At the same time, the voltage drop through the current path is monitored by an oscilloscope. For the wire-bonding sample, since the maximum temperature of the bond wire occurs on the bond point located on the die surface, only the temperature of the die and heatsink are considered.

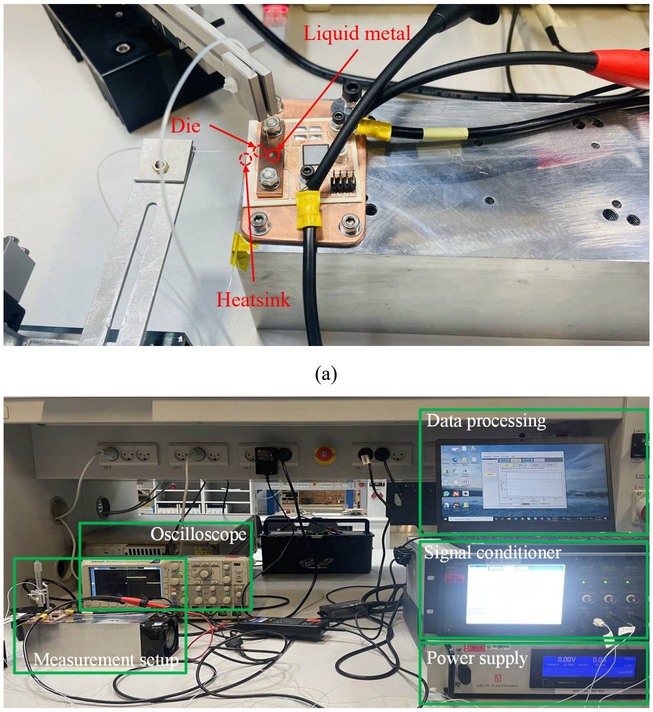

(a)

(b)

Fig. 3. Experiment setup, (a) measure positions of fiber optic temperature sensors, the dashed circles means perspectives, (b) measurement equipment.

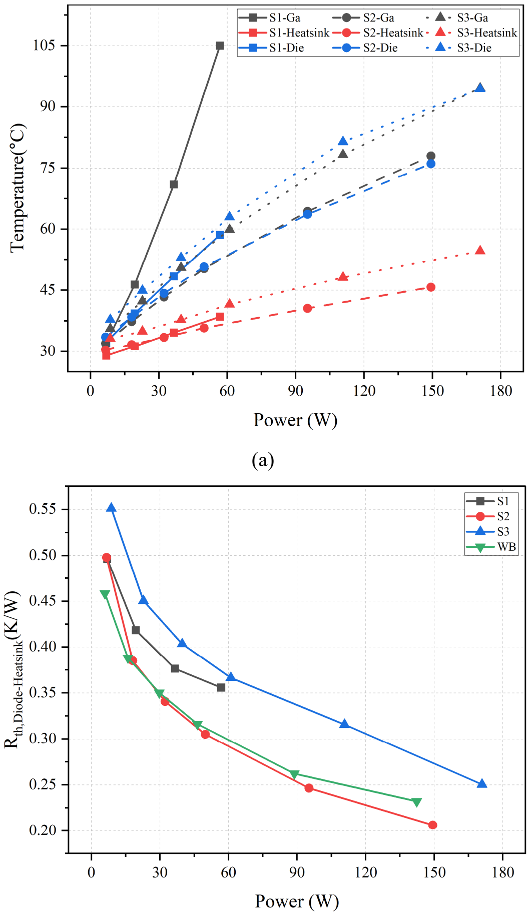

(a)

(b)

Fig. 4. (a) The temperature responses and (b) the thermal resistances from the diode die to the heatsink with different power dissipations.

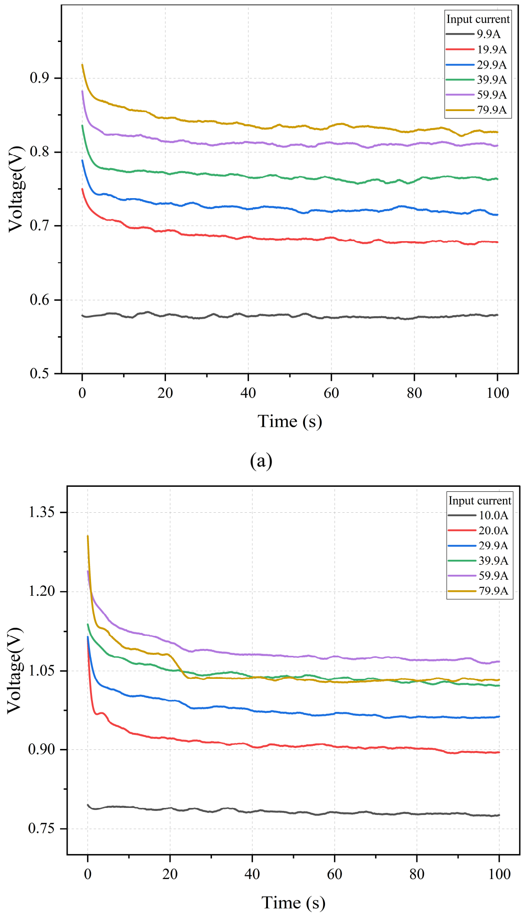

(a)

(b)

Fig. 5. The voltage drops through the current path of (a) sample 2, and (b) sample 3.

IV. RESULTS AND ANALYSIS

The temperature responses with different power dissipations of samples 1-3 are plotted in Fig. 4a. It can be seen that the gallium temperature of samples 2 and 3 is close to the diode die surface temperature, while the temperature of sample 3 is higher than sample 2, and the difference widens with increasing power dissipation. Furthermore, under the condition of similar heatsink temperature, the gallium temperature of sample 1 is much higher than that of other samples and also the surface temperature of the diode die itself. The phenomenon might be caused by the structural defects of the liquid material in sample 1 induced by insufficient fluidity and wetting conditions.

By applying (1), the thermal resistances at the time temperature getting stable from the die to the heatsink of all samples are characterized and compared in Fig. 4b. The highest curve suggests that poor heat dissipation occurs in the structure from the diode die to the heatsink of sample 3. However, in the absence of significant structural defects, because of the double-side cooling path offered by the copper busbar in the LM packaging configuration, the thermal characteristic of sample 2 is superior to the wire-bond module-sample 0, especially in the higher power stage.

Taking sample 2 and 3 as instances, the voltage drops through the current path are shown in Fig. 5, where the raw voltage data is recorded on the frequency of 100Msamples/s. To show the voltage trend clearly and remove the noise, a Savitzky-Golay filter with a window length of 3000 points was applied. In contrast with sample 2, the voltage drop in sample 3 is higher, thus causing greater conduction losses and resulting in higher die temperatures. Notably, in both samples 2 and 3, a slow decline in the forward voltage of the module can be observed in the initial stage, which can be an indication that also a self-healing ability of the LM exists. Under the action of the electric field and temperature field, the convective motion of LM contributes to better electrical properties.

V. SIMULATION VERIFICATION

For the abnormal temperature response observed in some LM interconnect samples, one hypothesis is that it is caused by insufficient liquid gallium filling level, and another hypothesis is that it is caused by possible structural defects. To verify them, a finite element simulation was developed as follows.

A. Model Configuration

The 3D model of the LM-interconnection module was built in Solidworks and shown in Fig. 6a. As for the LM modeling, the LM in well-packaged samples is considered to be sufficiently homogeneous to fill the injection holes of the busbar and the gap between the busbar and the die surface and is represented by the union of two cylinders, as shown in Fig. 6b. For saving computational time, a partial model containing the crucial parts of liquid gallium, diode die, busbar and corresponding packaging structures was separated from the full model and imported to ANSYS Workbench for finite element analysis.

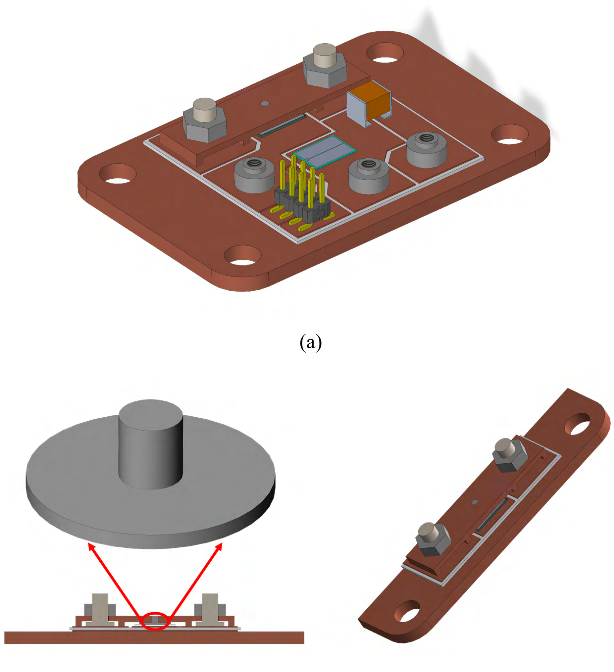
(a)

(b)

Fig. 6. 3D model of liquid metal interconnect module, (a) full model, (b) liquid metal model and partial model.

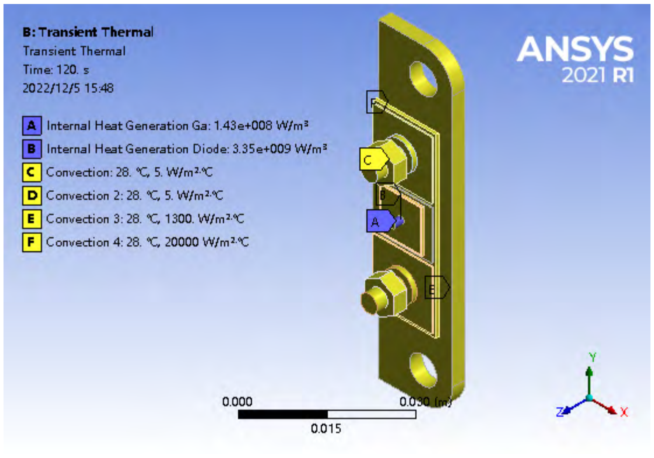
B: Transient Thermal
Transient Thermal
Time: 120. s
2022/12/5 15:48

A Internal Heat Generation Ga: 1.43e+008 W/m³
B Internal Heat Generation Diode: 3.35e+009 W/m³
C Convection: 28. °C, 5. W/m²·°C
D Convection 2: 28. °C, 5. W/m²·°C
E Convection 3: 28. °C, 1300. W/m²·°C
F Convection 4: 28. °C, 20000 W/m²·°C

Fig. 7. Simulation boundary conditions.

A 120s-transient thermal simulation consistent with the measurement was carried out to get the temperature responses, where the LM and the active region of the diode die were regarded as the thermal source due to the ohmic loss and conduction loss. The total power dissipation calculated from the experiment of sample 2 was distributed on these two parts in a ratio that changes with the input current. To compensate for the heat dissipation capacity of the removed part, a high convective heat transfer coefficient (*h*) of 20000W/m^{2}K was applied to the cross-section of the base, and *h* of 1300W/m^{2}K determined by experiment-based model correction was used on the bottom surface of the base for characterizing the heatsink. Other surfaces were cooled by natural convection (*h* of 5W/m^{2}K), and all boundary conditions are illustrated in Fig. 7.

During the post-processing stage, the maximum temperature of the LM top surface and the temperature of the node on the die surface near the edge position were extracted and compared with the experiment results of sample 2 in Fig. 8. With an average error of 3.7%, the configured FEA model and conditions were used in following simulations to investigate the abnormal thermal behavior.

B. Underfilling Simulation

The first hypothesis is that due to a poor wetting condition taking place at the diode die's metalized surface, the horizontal expansion of LM along the die surface is limited when injected into the power module through the hole of the busbar. As a result, the LM in the module can not sufficiently fill the gap between the busbar and the die surface as that in well-packaged samples. To describe this behavior, the bottom cylinder representing the LM between the busbar and diode die was contracted along the radial direction at four levels from the diameter of 6.2mm to the diameter of the injection hole. The diameters of the bottom cylinder at four levels were 6.2mm, 4.6mm, 3.1mm and 1.6mm, respectively, which equals volume shrink ratio of 0%, 35%, 59% and 73%. The corresponding models were updated in ANSYS Workbench directly by a parametric Solidworks input.

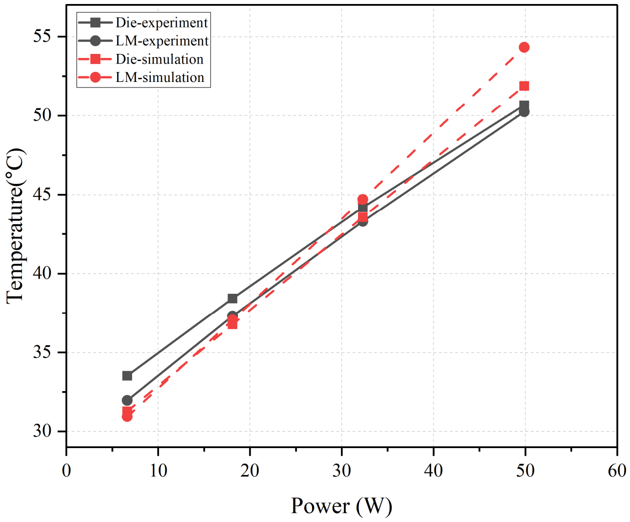

Fig. 8. Simulated and experimental temperatures as a function of power.

Maintaining the same diode die power losses as the sample with normal temperature responses when the input current stepped from 10A to 40A, a forward voltage drop of 20mV/°C on the diode die was considered, and the die power dissipation was further corrected by the temperature differences of sample 1 and 2 in the experiment. The power dissipation of LM was the total power calculated from the experiment of sample 1 minus the power loss of the die. Because of the volume shrinkage caused by the underfilling of the LM and hence the higher resistance of the LM, an increase in the LM power dissipation for the same input current was witnessed.

Following the same boundary conditions of the configured model, the simulation results in the case of insufficient filling are plotted in Fig. 9.

The temperature curves show that an underfill of the LM induced by the insufficient wet condition will increase power dissipation by increasing the resistance of the current path, causing the temperature of the LM to rise, and raising the junction temperature of the die slightly through heat transfer. With the increase of volume shrinkage, the temperature of LM and diode die are both higher and closer to the experiment results, but there is still a certain gap.

C. *Structural Defects Simulation*

Considering the temperature gap to the experiment results, another hypothesis is that, the abnormal increase in temperature is not only due to insufficient volume of gallium, but also structural defects, such as spots or interfaces where gallium does not wet the copper or die metallization surfaces sufficiently. This could likewise be interpreted as an increase in contact resistance. In the situation of least filled LM among the above cases (Φcylinder=1.6mm), the FEA model with structurally defective LM was built in ANSYS Mechanical where stochastically distributed spheres were generated and cut from the two cylinders by an APDL command to characterize the superficial and internal defects of LM. It should be noted that this is not an accurate visual representation of the gallium droplet, but is a way to simulate improper wetting and contact of surfaces, in which we also take into account the influence the variance in contact area has on the thermal resistance. Four defective models with volume porosity of 8.27%, 19.78%, 33.21% and 46.78% in this step and plotted in Fig. 10. In models with higher porosity, the voids with larger volume predominate. After the meshing operation, the .cdb files were imported into ANSYS Workbench to finish the analysis with the same boundary conditions as the above simulation. The simulation results are recorded in Fig. 11. It can be seen that as porosity increases, the temperature of LM and diode die both increase and reach up to the experiment temperature at the porosity of 46.78%.

These simulation results emphasize that the hypotheses put forward in this section that the structural defects in the LM could lead to the abnormal temperature response because of the local ohmic centralized self-heating as shown in Fig. 12 and increased power density.

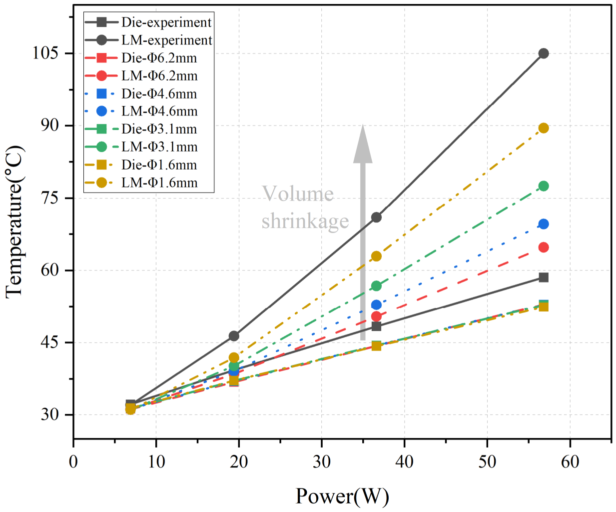

Fig. 9. Simulated and experimental temperatures as a function of power in the case of underfill.

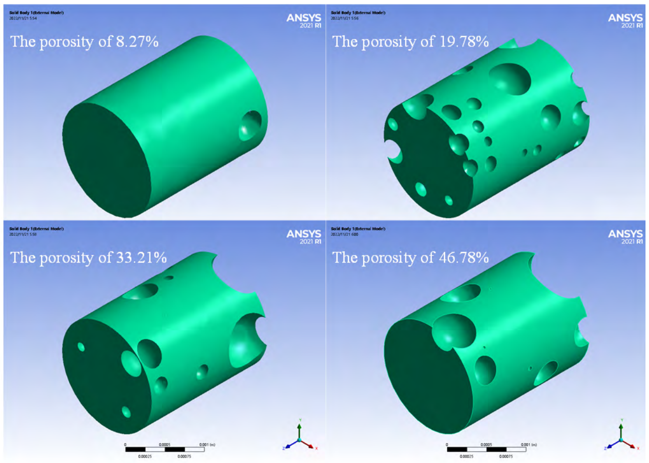

Fig. 10. The LM model with structural defects.

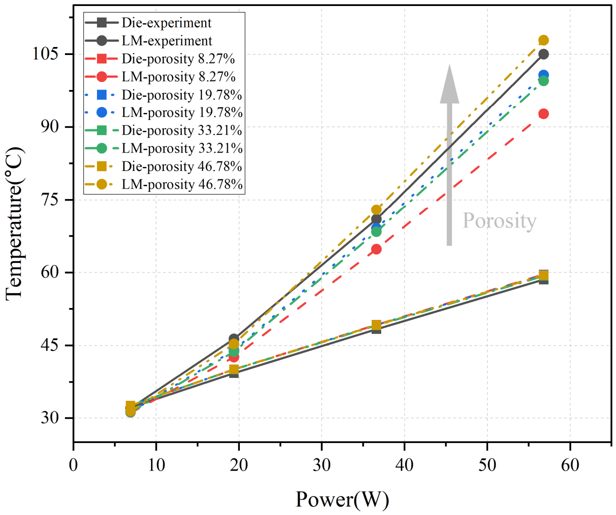

Fig. 11. Simulated and experimental temperatures as a function of power in the case of structural defects.

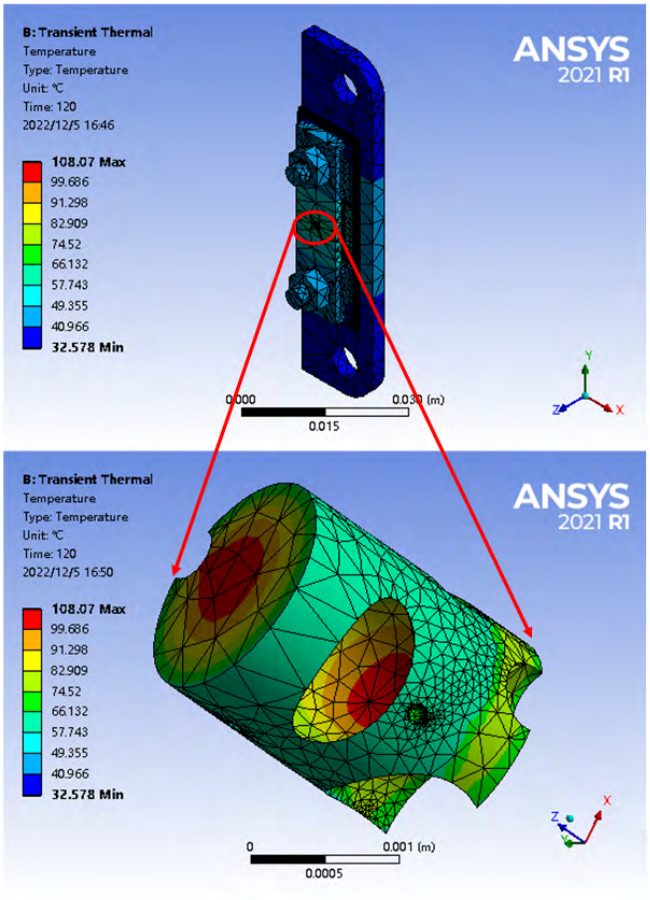

Fig. 12. Temperature distribution and local temperature concentration.

VI. Conclusions

This paper has investigated a liquid metal (LM) interconnection technique for power semiconductors and compared it with a traditional wire-bonded module. From the aspect of thermal resistance, it was found that a LM interconnection module has slightly better thermal characteristics, with a thermal resistance of 0.21 K/W at a power dissipation of 150 W, where the wire-bond module had 0.24 K/W, indicating a possible reduction of 12.5% in thermal resistance. However, due to the difficulty in achieving consistent packaging of the LM module, other samples performed worse than the wire-bonded module.

It is concluded that with a proper packaging process and fewer structural defects, the LM interconnects method can improve the thermal behavior of power semiconductors by offering a better heat dissipation capability and lower operation temperature, as a result, prolonging the lifetime in use, in addition to removing the fundamental failure mode of bond wire failure in power semiconductors. Besides, the decline in the forward voltage of the module suggests a self-healing ability of LM, which also benefits the thermal behavior of LM interconnections for power semiconductors during prolonged use.

A finite element simulation investigating the possible reasons for the abnormal temperature responses confirms the hypothesis that the underfill and structural defects of interconnect liquid material induced by insufficient wetting condition and fluidity will lead to increasing the resistance of the current path and local ohmic centralized self-heating, hence getting a higher operation temperature.

The findings here about the thermal characteristics provide evidence supporting the application of LM interconnections for power semiconductors, and also put forward the challenges of large-scale industrial applications with a stable and mature packaging process. As the starting stage of research on LM interconnects for power semiconductors, improved LM interconnect structures will be investigated to accelerate their consistent and reliable use in industrial applications.

References

[1] M. R. Choudhury and K. Debnath, “Current and future trends in micro-joining and nano-joining,” in Woodhead Publishing Reviews: Mechanical Engineering Series, Joining Processes for Dissimilar and Advanced Materials, Duxford: Woodhead Publishing, 2022, pp. 209–239.

[2] K. B. Pedersen and K. Pedersen, “Bond wire lift-off in IGBT modules due to thermomechanical induced stress,” in: 2012 3rd IEEE International Symposium on Power Electronics for Distributed Generation Systems, PEDG 2012, 2012, pp. 519–526.

[3] Y. Wang, J. Guo, W. Xiao, K. Sun, H. Wang, and L. Hu, “Recent Development of Liquid Metal-Based Functional Materials Combined with Common Transition Metals,” Adv. Mater. Interfaces, vol. 8, no. 24, pp. 1–17, 2021.

[4] N. Baker, “Use of Liquid-Metal as the Frontside Interconnect in Power Semiconductors,” presented in: IEEE International Workshop on Integrated Power Packaging, IWIPP 2022,2022.

[5] C. Majidi, “Mechanics of fluid-elastomer systems in soft robotics,” in Woodhead Publishing in Materials, Robotic Systems and Autonomous Platforms, Duxford: Woodhead Publishing, 2019, pp. 425–448.

[6] A.B. Jorgensen, T.H. Cheng, D. Hopkins, S. Beczkowski, C. Uhrenfeldt, and S. Munk-Nielsen, “Thermal characteristics and simulation of an integrated GaN eHEMT power module,” in: 2019 21st European Conference on Power Electronics and Applications,2019.